Received 3 October 2025; Accepted 9 December 2025
https://doi.org/10.48612/letters/2026-1-64-70
https://elibrary.ru/gozeej

Modeling the magnetic properties of cobalt nanofilms as promising materials for spintronics devices

A. Yu. Fedotov[1], O. Yu. Severyukhina[†1], A. Yu. Salomatina[1], A. S. Sidorenko[2,3]

[†]sevol@udman.ru

[1]Udmurt Federal Research Center of the Ural Branch of the Russian Academy of Sciences, Izhevsk 426067, Russia
[2]Technical University of Moldova, Chisinau MD-2004, Moldova
[3]Moscow Institute of Physics and Technology, Moscow region, Dolgoprudny 141701, Russia

Abstract: A hybrid molecular dynamics and spin modeling approach using the SPIN package within the LAMMPS software suite was employed to investigate the influence of thickness on the magnetic properties of crystalline cobalt nanofilms with a face-centered cubic structure. Film thickness acts as a critical parameter determining magnetic behavior through the dynamic interplay of surface and bulk effects. In the region of ultrathin films (thickness less than 4.5 nm), a pronouncedly inhomogeneous magnetic response is observed, stemming from the dominance of surface effects. Key contributing factors include the influence of atomic-scale roughness, which creates local demagnetizing fields. This leads to complex domain wall dynamics, manifested as abrupt changes in magnetization and fine-scale non-uniformity in its spatial distribution. When the film thickness exceeds 4.5 nm, a transition to bulk-like behavior occurs. The reduction in the relative proportion of surface atoms allows the bulk properties of cobalt to come to the fore. Consequently, the dependence of magnetization on the external field becomes more pronounced and stable, while its spatial distribution exhibits increased uniformity. The normalized magnetic energy stabilizes at a level characteristic of the bulk material. The obtained results hold practical significance for the design of spintronics and magnetic recording devices. Furthermore, by understanding the magnetic interactions and dynamic responses of nanofilms, researchers and engineers can develop more efficient and reliable magnetic memory technologies, as well as novel spintronic components that leverage their unique magnetic characteristics for applications in sensing, data processing, and quantum information systems.

Keywords: nanofilms, magnetic fields, mathematical modeling, molecular dynamics, spin dynamics, ferromagnets

Acknowledgements: *The work was carried out within the framework of the state assignment of the Ministry of Science and Higher Education of the Russian Federation (topic No. FUUE-2025-0001 "Modeling and experimental studies of the structure and magnetic parameters of a Josephson contact made of a multilayer nanostructure", state registration No. 125020501412-9) and with the financial support of the Russian Science Foundation (project No. 23-72-30004) and the project No. 020201 of the Moldova State Program "Nanostructures and advanced materials for implementation in spintronics, thermoelectricity and optoelectronics".*

1. Introduction

The practical significance of using cobalt nanostructures is due to their unique physico-chemical properties, which open new possibilities for applications in various fields. Cobalt nanofilms are widely used in electronics [1,2] because of their good conductive properties and ability to form thin layers, making them ideal for creating new functional devices such as sensors [3,4], batteries and fuel cells [5], and solar panels [6,7]. The unique electrical and mechanical properties of cobalt-based nanomaterials can improve energy storage efficiency and increase battery lifespan. Studies [8,9] show that cobalt can balance and enhance the conductivity and stability of electrodes, which is an important factor for improving the performance of lithium-ion batteries.

Cobalt nanofilms exhibit interesting and unconventional magnetic properties, making them promising for use in magnetic devices and information technologies [10–12]. These materials can be used in the production of hard drives and magnetic recording devices, which is highly relevant in the context of increasing data volumes and the need for efficient information storage systems. Cobalt nanostructures play a significant role in spintronics [13,14], which explores the possibility of using not only charge but also electron spin for storing and processing information. Cobalt has high magnetic coherence and can form ferromagnetic nanostructures [15–17]. These structures can be created as films, dots, or wires and are often used in devices such as magnetoresistive memory types, spin transistors, and communication systems. One of the key advantages of cobalt nanostructures is the ability to manipulate electron spin at relatively low energy costs. This opens prospects for creating more efficient and faster devices. Additionally, cobalt can be combined with other materials [18–20],

significantly improving the characteristics of spintronic devices.

Thanks to its unique magnetic properties and ability to provide high control over spin polarization, cobalt nanostructures are used in Josephson contacts [21,22]. Josephson contacts, which are one of the key elements in superconducting technologies, utilize tunneling effects between two superconducting materials, enabling the creation of devices for high-frequency electronics, quantum computing, and sensors.

Cobalt in the form of nanostructures is also used to generate spin-polarized currents [23,24], increasing the sensitivity and efficiency of Josephson contacts. Due to their ferromagnetic nature, cobalt nanostructures enable control over electron spin, which is critically important for developing new types of contact structures known as spin Josephson contacts. Using cobalt in these contacts can improve their characteristics such as critical current magnitude and resistance to thermal fluctuations [25]. Moreover, cobalt nanostructures can be easily integrated into existing technologies due to their compatibility with various superconductors (materials or devices with outstanding electrical properties such as high conductivity, low resistance, or special properties in magnetic fields).

The aim of this work is to study the magnetic behavior of thin cobalt films under external magnetic fields of varying strength. The direction of the external field induction was chosen perpendicular to the plane of the nanofilms. The thicknesses of the cobalt films varied. This work builds upon earlier publications by the authors that investigated the structure, composition, and morphology of composites with cobalt nanofilms [26–28], as well as analyzed their magnetic properties [29].

2. Mathematical model and problem statement

The physical system under study consists of crystalline cobalt nanofilms with a face-centered cubic (FCC) structure, with thicknesses varying in the nanometer range (from 1.8 to 7.1 nm). The key objective is to study the influence of film thickness, a critical parameter, on its magnetic properties at room temperature. The external magnetic field is directed perpendicular to the film plane, and its magnitude varies from 0 to 3 T.

The physical formulation of the problem involves establishing quantitative and qualitative relationships between nanofilm thickness, the fraction of surface atoms, the magnitude of the external magnetic field, and the resulting magnetic characteristics (magnetization and magnetic energy). This is necessary for predicting the behavior of promising materials in spintronic devices.

For the computational experiments in this work, a combined mathematical model of molecular dynamics and spin reorientation calculations of atoms [30] was used. This model integrates the equations of molecular dynamics, which describe the motion of atoms and molecules in the system, with methods that account for the spin states of particles. This allows for the analysis of both classical interaction forces and quantum effects related to spins, which is especially important when studying ferromagnets, antiferromagnets, and other magnetic systems.

The foundation of the employed mathematical model consists of the Langevin equation [31] and the Landau–Lifshitz–Gilbert equation [32]:

$$m_i \frac{d^2\mathbf{r}_i}{dt^2} = -\frac{\partial U_{\text{MEAM}}(\mathbf{r})}{\partial \mathbf{r}_i} - \frac{\partial H_{\text{mag}}(\mathbf{r},\mathbf{s})}{\partial \mathbf{r}_i} - \kappa \frac{d\mathbf{r}_i}{dt} + \boldsymbol{\chi}(t), \tag{1}$$

$$\frac{d\mathbf{s}_i}{dt} = \frac{1}{(1+\lambda^2)}\Big((\boldsymbol{\omega}_i + \boldsymbol{\eta}(t)) \times \mathbf{s}_i + \lambda \mathbf{s}_i \times (\boldsymbol{\omega}_i \times \mathbf{s}_i)\Big), \quad i = 1,2,\ldots,N, \tag{2}$$

$$H_{\text{mag}}(\mathbf{r},\mathbf{s}) = -\sum_{i,j,i\neq j}^{N} J(r_{ij})\mathbf{s}_i \cdot \mathbf{s}_j - \mu_B \mu_0 \sum_{i=0}^{N} g_i \mathbf{s}_i \cdot \mathbf{B}_{\text{ext}}, \quad \boldsymbol{\omega}_i = -\frac{1}{\hbar}\frac{\partial H_{\text{mag}}}{\partial \mathbf{s}_i}, \tag{3}$$

where $H_{\text{mag}}(\mathbf{r},\mathbf{s})$ — the energy of magnetic interaction of the atomic system, depending on the position vectors of all atoms $\mathbf{r} = \{\mathbf{r}_1, \mathbf{r}_2, ..., \mathbf{r}_N\}$ and their spin orientations $\mathbf{s} = \{\mathbf{s}_1, \mathbf{s}_2, ..., \mathbf{s}_N\}$; $U_{\text{MEAM}}(\mathbf{r})$ — the potential energy of force interaction; κ — the viscous damping parameter; λ — the spin damping coefficient; $\hbar$ — the reduced Planck constant; $J(r_{ij})$ — the exchange integral value, which regulates the magnetic ordering of spins depending on the distance between atoms $r_{ij}=|\mathbf{r}_j - \mathbf{r}_i|$; $\mathbf{B}_{\text{ext}}$ — the external magnetic field induction; g_i — the Landé g-factor for the i-th atom; μ_0 — the magnetic constant; μ_B — the Bohr magneton. The exchange integral was described as a Bethe–Slater curve and included three parameters to reflect the degree of magnetic interaction between the spins of atoms:

$$J(r_{ij}) = 4\alpha\left(\frac{r_{ij}}{\delta}\right)^2\left(1-\gamma\left(\frac{r_{ij}}{\delta}\right)^2\right)e^{-\left(\frac{r_{ij}}{\delta}\right)^2}\Theta(R_c - r_{ij}), \quad i,j = 1,2,\ldots,N_{\text{atom}}, \tag{4}$$

where α, δ, γ are the three constant coefficients, and R_c is the radius cutoff associated to the pair interaction.

To describe the motion of atoms and their magnetic moment dynamics, functions $\boldsymbol{\chi}(t)$ and $\boldsymbol{\eta}(t)$ are used, representing white noise and depending on the values of thermodynamic and spin temperatures of atoms [33].

For modeling force interactions between atoms, a potential based on the Modified Embedded Atom Method (MEAM) was used — $U_{\text{MEAM}}(\mathbf{r})$. MEAM is an important tool in quantum chemistry and molecular dynamics because it is based on the distribution of electronic density in atoms and molecules and allows accounting for the influence of neighboring atoms on electrons, which is especially important in studying molecular structures and their properties. The application of MEAM assumes that instead of a point approximation for electron-nucleus interactions, an environmental description with various characteristics is considered, significantly simplifying computational processes during mathematical calculations [34]. The method is widely used in developing new materials and investigating their properties. Additionally, MEAM has proven effective when combined with other methods, such as density functional theory, to obtain a more comprehensive and accurate picture of interactions in complex multi-atomic systems.

The interaction between the coordinate subsystem (Eq. (1)) and the spin subsystem (Eq. (2)) in the model was implemented through an exchange integral $J(r_{ij})$. This integral reflects the degree of influence between neighboring atomic spins and directly affects the magnetic properties of the material. In the employed model, the exchange integral was described using a Bethe–Slater curve and included three parameters to reflect the degree of magnetic interaction between atomic spins. When describing magnetic interactions in solids, this exchange integral and its parameters play a key role because they directly influence atomic spin distribution, determine various orbital states depending on electronic structure, and shape the type of magnetic behavior of the studied material (ferromagnetic, antiferromagnetic, paramagnetic, etc.). A more detailed mathematical model, types of magnetic interactions, expressions for the exchange integral, and details about MEAM are described in works [28 – 30].

The mathematical model used is implemented within the freely available LAMMPS software package [35], which allows simulating various physical and chemical processes at atomic and molecular levels. The SPIN package [30] within LAMMPS specializes in modeling magnetic materials and spin systems. The SPIN module provides tools for working with atomic magnetic moments, enabling studies of magnetic system behavior under different conditions such as temperature, interactions, and external magnetic fields. It supports various models of magnetic interactions, allowing exploration of complex phenomena like ferromagnetism, antiferromagnetism, spin waves, spin dynamics, and phase transitions in magnetic systems.

In this work, cobalt crystalline nanofilms with a face-centered cubic (FCC) structure were considered. The films contained 20 elementary cells along x and y axes. Along z-axis, their thickness varied from 5 to 20 elementary cells with a step size of 1 cell. Computational experiments were conducted where film thicknesses varied so that studied systems contained from 8 800 to 32 800 atoms. During each simulation, an external magnetic field remained constant within each run but varied between runs from 0 to 3 T. Periodic boundary conditions were applied along horizontal axes (x and y) at both edges of the nanofilm, while boundary conditions along vertical axis (z) remained free. An illustration of the modeled system is shown in Fig. 1.

Each calculation consisted of two stages. In the first stage, the system underwent a phase of initial partial self-organization of the magnetic moments. At the initial moment in time, the atomic spins were randomly oriented according to their spin temperature of 300 K. Subsequently, over a period of 50 ps, the system relaxed under conditions of no external forces and in a constant magnetic field. This stage was necessary to eliminate the influence of initial conditions on the analyzed magnetic characteristics. In the second stage, lasting 10 ps, the study of magnetic properties continued, and graphical dependencies were constructed for them. During both stages, the thermodynamic and spin temperatures were maintained at 300 K with damping coefficients of temperature $\tau_t = \tau_s = 0.01$ ps. The integration step in the computational experiments was $dt = 0.1$ fs.

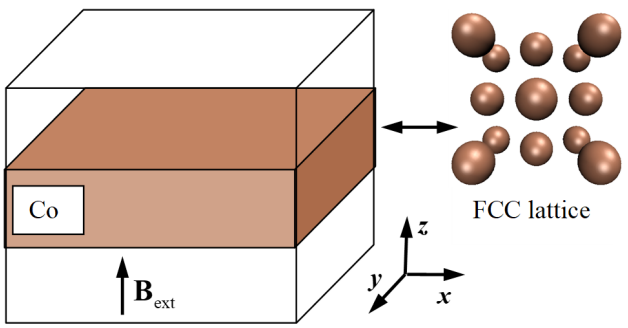

Fig. 1. (Color online) The appearance of the computational domain in the study of magnetic properties of crystalline cobalt nanofilms.

3. Results and discussion

As a result of conducting a series of computational experiments, the behavior of atomic spins in cobalt nanofilms of various thicknesses under a constant external magnetic field $\mathbf{B}_{ext} = 0 - 3$ T was analyzed. Visually, the obtained images of spin vector distributions indicated the formation of magnetic domains with sizes ranging from one to several tens of nanometers. In thicker films and at larger spatial scales, domain walls between uniformly oriented regions became clearly visible. The obtained data are in good agreement with studies [12], where the structure of magnetic domains in cobalt nanofilms grown by molecular beam epitaxy was analyzed. Additionally, in [12], it is shown that as the thickness of the nanofilm increases, the magnetization changes from being completely planar with perpendicular orientation to being out-of-plane relative to the film surface.

Based on the distribution of atomic magnetic moments, the coordinates and magnitude of the magnetization vector of the nanofilm were calculated. After the relaxation stage, the magnitude of the magnetization vector changed insignificantly within a few percent, so its dependence on time is not presented in this work. Greater interest is in the value of the magnetization magnitude for cobalt nanofilms of different thicknesses in an external magnetic field. The presented value of the magnetization magnitude as a function of the crystalline layer thickness L_z is shown in Fig. 2 a. This value (ranging from 0 to 1) was used for convenience in comparing data, to eliminate dependence of the total magnetization on the number of atoms. The average value of the magnetization magnitude for different external magnetic induction values is shown in Fig. 2 b. The colors in Fig. 2 a and Fig. 2 b correspond to each other.

An analysis of the spatial distribution of magnetic moments revealed the formation of a domain structure with a predominance of perpendicular magnetization orientation in ultrathin films (<4.5 nm) and a transition to plane-oriented domains with increasing thickness. The observed domain walls in the bulk of the films corresponded to the Bloch type. The presented values of the magnetization modulus were calculated as the modulus of the magnetization vector averaged over the entire film volume, which correctly characterizes the overall magnetic response of the system even in the presence of domains with different directions.

From the analysis of the graphs in Fig. 2, it is evident that the magnitude of magnetization in cobalt nanofilms of different

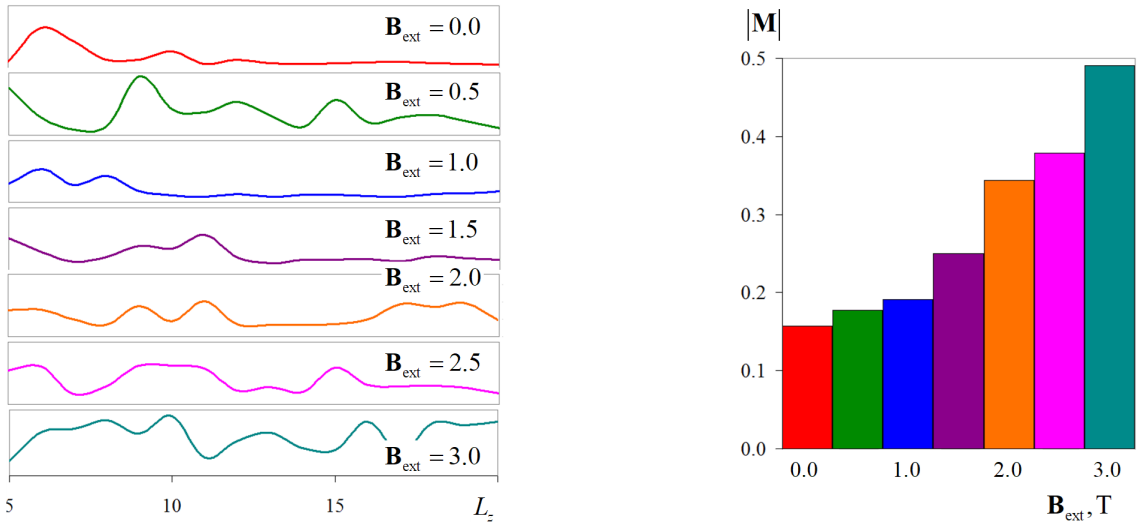

Fig. 2. (Color online) Variation of the normalized magnetization magnitude depending on the thickness of the crystalline layers of the cobalt nanofilm L_z (a), and the average value of the normalized magnetization magnitude (b) in an external magnetic field of different strengths.

thicknesses behaves unevenly. Spikes and fluctuations in the total magnetization are observed, which may be associated with the movement of domain walls within the nanomaterial. Such behavior is likely a direct consequence of the dominant influence of surface effects and microstructural features at the nanoscale. A key role in this case is played by surface (interfacial) magnetic anisotropy (PMA) [36, 37], whose intensity is inversely proportional to the film thickness. In thin films, PMA becomes so strong that it creates energy barriers stabilizing domains with perpendicular magnetization. Uneven pinning of domain walls at surface defects or interface inhomogeneities (for example, with the substrate or protective layer) can lead to their "jump-like" movement under an external field. Each such jump, accompanied by switching of magnetic moments in a group of domains, manifests on the magnetization graph as a sharp spike or drop.

Additionally, surface roughness significantly contributes to the total magnetization. Atomic irregularities, growth islands, or grain boundaries create local inhomogeneities in the magnetic field — demagnetizing fields. These fields act as traps or barriers for domain walls [37]. When the external field changes, a domain wall can be held between such inhomogeneities until the applied field exceeds a critical value for its depinning, which also results in a sudden change in magnetization. This effect is exacerbated as the film thickness decreases, when roughness becomes comparable to its size.

Nevertheless, the behavior of the histogram in Fig. 2b indicates a directly proportional dependence of the average value of the magnetization magnitude on the external magnetic induction. The averaging of the magnetization magnitude was performed over all film thicknesses. The dependence shown in Fig. 2b has a nonlinear character with a stronger correlation between these quantities as their values increase. This feature is explained by fundamental mechanisms of hysteresis in nanomaterials and by an increased influence of surface effects within certain field ranges. The proportion of surface atoms depending on the thickness of the crystalline layers of cobalt nanofilm is shown in Table 1.

It is known that surface effects in nanofilms can be a determining factor in the material's functionality [38, 39]. This occurs due to a sharp increase in the surface-to-volume ratio, as a significant proportion of atoms are located at the boundary with another coating or the surrounding environment. The breaking of the crystal lattice symmetry at the surface leads to a reconstruction of the electronic orbitals of cobalt atoms. This generates a strong surface magnetic anisotropy (PMA), sometimes manifesting as perpendicular magnetic anisotropy. The effect is especially pronounced at cobalt interfaces with heavy metals (Pt, Pd) or oxides (MgO, Al_2O_3), where it depends heavily on the crystal structure of cobalt and the quality of the boundary.

In addition to anisotropy, surface effects influence the very magnitude of magnetization, as shown in Fig. 2b. Atoms at the boundary may possess a magnetic moment different from that of atoms within the volume due to altered hybridization of electronic states or structural defects. The weakening of exchange interactions among surface atoms due to the lack of neighbors can also lead to a reduction in the Curie temperature of the nanofilm compared to bulk cobalt. Moreover, surfaces and interfaces become primary sources of spin relaxation, increasing energy losses and affecting the speed of magnetization reversal during dynamic processes.

Continuing the analysis, Fig. 3 presents the distribution of normalized magnetization magnitude for cobalt nanofilms of various thicknesses under an external magnetic field. The film thicknesses in Table 1 are given in nanometers, ranging from 1.8 to 7.1 nm. The color palette on the right corresponds to the normalized magnetization magnitude of the samples,

Table 1. The proportion of surface atoms depending on the thickness of the cobalt nanofilm.

Nanofilm thickness, unit cells	5	6	7	8	9	10	11	12	13	14	15	16	17	18	19	20
Proportion of surface atoms, %	12	11	9	8	7	7	6	6	5	5	5	4	4	4	4	3

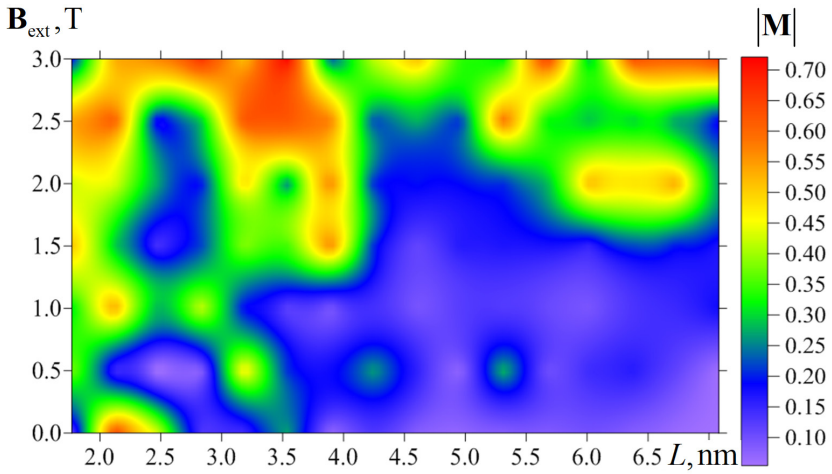

Fig. 3. (Color online) Distribution of the normalized magnetization magnitude for cobalt nanofilms of various thicknesses under an external magnetic field.

which varied from 0 to 0.7 in computational experiments. Interpreting this color palette (corresponding to normalized magnetization values from 0 to 0.7) allows for a deeper understanding of the processes occurring. Areas with low values (close to zero, "cold" colors) correspond to regions with very weak or zero magnetization magnitude. Such zones are characteristic of domain wall centers, strongly demagnetized regions at the beginning of magnetization reversal processes, and prominently expressed areas near the surface. High values (close to 0.7, "warm" colors) indicate regions saturated or nearly saturated with magnetization. Color gradients on the map visualize transitional states of magnetization during exposure to an external field.

The modeling results presented in Fig. 3 clearly demonstrate a significant difference in the magnetic response of the films depending on their thickness. The behavior of ultrathin cobalt films (less than 4.5 nm thick) is characterized by a pronounced dependence of the magnetization magnitude on the external magnetic field. This high sensitivity is explained by the dominant influence of surface effects. A substantial proportion of regions with disrupted exchange interactions and interface effects significantly affect the average magnetization of the entire film. At the same time, strong perpendicular magnetic anisotropy (PMA) may require applying considerably larger fields to achieve saturation of magnetization along the easy axis. An additional complexity arises from the inhomogeneity of the magnetization reversal process: the combination of strong PMA, inevitable surface roughness, and interface defects contributes to the formation of a complex domain structure, which is reflected in a colorful pattern of magnetization distribution on the map. PMA results from a decrease in the symmetry of the crystal field for surface atoms, which is accounted for through the dependence of the exchange integral on the local interatomic environment. Atomic roughness is formed by thermal vibrations of surface atoms (the Langevin equation with stochastic force) and lattice relaxation at the free boundary.

Moving to thicker films (range 4.5 – 7.1 nm), a significant change in the nature of the dependence of magnetization on the field is observed. The dependence becomes more pronounced and well-defined. This is associated with a weakening of the relative contribution of surface effects as the surface-to-volume ratio decreases. The influence of surface zones and interface-induced PMA becomes less significant against the background of increasing importance of bulk magnetic properties of cobalt. The volume exchange interaction and its characteristic ferromagnetic behavior dominate for bulk cobalt. As a result, the magnetic response of the film becomes more rigid. The magnetization reversal process proceeds more coherently and uniformly throughout the material volume. Although a domain structure is present, its scale and impact on the overall response become more predictable and approach that of bulk material, which is reflected in larger, more homogeneous regions on the magnetization distribution map.

Another important characteristic for the studied cobalt nanofilms is their magnetic energy. For convenience, this energy was normalized relative to the total number of atoms in the film. The graphs showing changes in average magnetic energy depending on the fraction of surface atoms (plot with triangular markers) and film thickness (reduced area at the bottom) are presented in Fig. 4. The dependence of normalized magnetic energy on surface atom fraction demonstrates a pronounced linear trend, well approximated by a straight line. This is a direct consequence that surface atoms contribute significantly different, usually higher, amounts to the total magnetic energy compared to atoms within the volume of the film. Each additional surface atom adds its characteristic share of energy associated with disrupted coordination, altered electronic structure, surface anisotropy, and influence from neighboring materials at interfaces. The form of the approximating linear function and the magnitude of approximation error are shown directly on the graph within a highlighted frame.

Unlike this, the dependence of normalized magnetic energy on film thickness has a nonlinear character. The observed nonlinearity is explained by the changing relative contribution of surface effects as the thickness increases. In ultrathin films (with small thickness), the fraction of surface atoms is maximal, and their contribution to the total magnetic energy dominates. However, as the film thickness grows, the ratio of surface area to volume decreases (see Table 1). As a

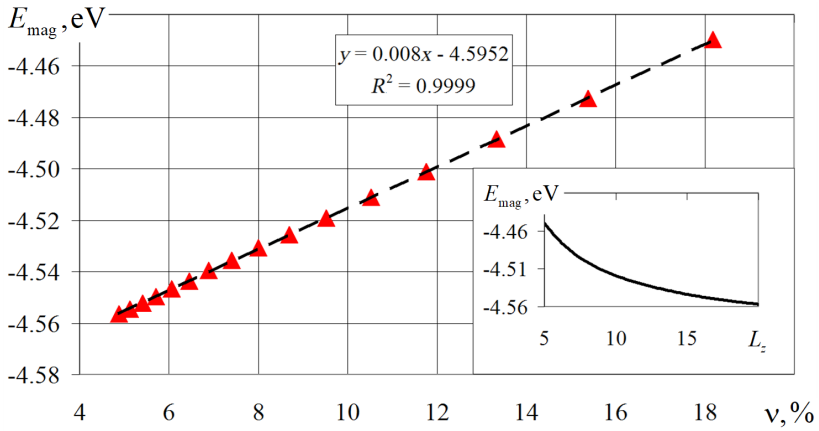

Fig. 4. (Color online) Variation of the average magnetic energy depending on the fraction of surface atoms and the thickness of cobalt nanofilms (inset).

result, after reaching a certain thickness (where the surface contribution becomes relatively small), the normalized magnetic energy approaches a value close to the steady-state energy corresponding to bulk cobalt. Further increases in thickness lead to only minor changes in energy, since the properties of the film increasingly resemble those of bulk material, where the influence of surface effects diminishes.

The established universal linear relationship between the normalized magnetic energy and the fraction of surface atoms serves as direct evidence of the crucial role of interfaces as sources of increased energy and magnetic inhomogeneity in nanomaterials [40, 41]. The movement of domain walls, their pinning at defects, inhomogeneities, and modified surface areas, leads to a discrete rather than smooth magnetization reversal process.

4. Conclusion

The comprehensive modeling of cobalt nanofilms using a hybrid molecular and spin dynamics method revealed a fundamental dependence of magnetic properties on the material's thickness, driven by the balance between surface and volume effects. The employed model allows for describing the dynamics of magnetic states at various temperatures and conditions, as well as investigating mechanisms of magnetization and magnetic behavior in nanomaterials.

In the ultrathin range (less than 4.5 nm), the magnetic behavior of nanofilms differs radically from bulk cobalt, exhibiting pronounced inhomogeneity. The key factor here is the dominance of surface effects and strong interface-induced PMA generated at the interfaces. As the film thickness increases to 4.5 – 7.1 nm, a transition to volume-like behavior is observed. Consequently, the dependence of magnetization on an external field becomes more pronounced and stable, while the spatial distribution of magnetization shows increased homogeneity and larger magnetic domains, indicating cooperative magnetization reversal processes.

From a practical standpoint, these results can be utilized in designing spintronic devices and magnetic storage systems. Ultrathin films (less than 4.5 nm) are promising for memory elements (STT-MRAM) due to their strong PMA but require careful engineering of interfaces and protection against degradation to minimize adverse surface effects. Films with thicknesses between 4.5 – 7.1 nm offer predictable volume-like behavior, which is optimal for applications sensitive to magnetization uniformity. Managing the relationship between film thickness and surface effects opens pathways for targeted development of cobalt nanofilms with tailored magnetic properties for quantum electronics and advanced nanotechnologies.

References

1. J. O. Emegha, K. Onyenike, R. O. Jolayemi, et al., Synthesis and characterization of zinc cobalt sulphide nanofilms for optoelectronic applications, Chemistry of Inorganic Materials 4 (2024) 100068.
2. M. Reinhardt, S. Dalgleish, Y. Shuku, et al., Molecular and thin film properties of cobalt half-sandwich compounds for optoelectronic application, Physical Chemistry Chemical Physics 19, 9 (2017) 6768 – 6776.
3. J. Wöllenstein, M. Burgmair, G. Plescher, et al., Cobalt oxide based gas sensors on silicon substrate for operation at low temperatures, Sensors and Actuators B: Chemical 93, 1 – 3 (2003) 442 – 448.
4. B. C. Yadav, R. C. Yadav, S. Singh, et al., Nanostructured cobalt oxide and cobalt titanate thin films as optical humidity sensor: a new approach, Optics & Laser Technology 49 (2013) 68 – 74.
5. Y. Q. Chu, Z. W. Fu, Q. Z. Qin, Cobalt ferrite thin films as anode material for lithium ion batteries, Electrochimica Acta 49, 27 (2004) 4915 – 4921.
6. J. S. Kang, J. Y. Kim, J. Yoon, et al., Room-Temperature Vapor Deposition of Cobalt Nitride Nanofilms for Mesoscopic and Perovskite Solar Cells, Advanced Energy Materials 8, 13 (2018) 1703114.
7. A. Kaphle, P. Hari, Enhancement in power conversion efficiency of silicon solar cells with cobalt doped ZnO nanoparticle thin film layers, Thin Solid Films 657 (2018) 76 – 87.
8. K. K. Lee, W. S. Chin, C. H. Sow, Cobalt-based compounds and composites as electrode materials for high-performance electrochemical capacitors, Journal of Materials Chemistry A 2, 41 (2014) 17212 – 17248.
9. F. Zhao, Y. Wang, X. Xu, et al., Cobalt hexacyanoferrate nanoparticles as a high-rate and ultra-stable supercapacitor

electrode material, ACS applied materials & interfaces 6, 14 (2014) 11007–11012.
10. D. Schmidt, A.C. Kjerstad, T. Hofmann, et al., Optical, structural, and magnetic properties of cobalt nanostructure thin films, Journal of Applied Physics 105, 11 (2009) 113508.
11. S. Martins, J. de Rojas, Z. Tan, et al., Dynamic electric-field-induced magnetic effects in cobalt oxide thin films: towards magneto-ionic synapses, Nanoscale 14, 3 (2022) 842 – 852.
12. M. Hehn, S. Padovani, K. Ounadjela, J.P. Bucher, Nanoscale magnetic domain structures in epitaxial cobalt films, Physical Review B 54, 5 (1996) 3428.
13. K.P. Bhatti, V.K. Malik, S. Chaudhary, Cobalt substituted ZnO thin films: a potential candidate for spintronics, Journal of Materials Science: Materials in Electronics 19 (2008) 849 – 854.
14. T. Wen, K.M. Krishnan, Cobalt-based magnetic nanocomposites: fabrication, fundamentals and applications, Journal of Physics D: Applied Physics 44, 39 (2011) 393001.
15. D. Srikala, V.N. Singh, A. Banerjee, B.R. Mehta, S. Patnaik, Synthesis and characterization of ferromagnetic cobalt nanospheres, nanodiscs and nanocubes, Journal of nanoscience and nanotechnology 9, 9 (2009) 5627 – 5632.
16. C.L. Londoño-Calderón, O. Moscoso-Londoño, D. Muraca, et al., Synthesis and magnetic properties of cobalt-iron/cobalt-ferrite soft/hard magnetic core/shell nanowires, Nanotechnology 28, 24 (2017) 245605.
17. J. Zhao, M. Spasova, Z. A. Li, M. Zharnikov, Ferromagnetic cobalt nanoparticles and their immobilization on monomolecular films and chemical templates, Advanced Functional Materials 21, 24 (2011) 4724 – 4735.
18. V. P Senthil., J. Gajendiran, S.G. Raj, et al., Study of structural and magnetic properties of cobalt ferrite ($CoFe_2O_4$) nanostructures, Chemical Physics Letters 695 (2018) 19 – 23.
19. V. Repain, G. Baudot, H. Ellmer, S. Rousset, Two-dimensional long-range–ordered growth of uniform cobalt nanostructures on a Au(111) vicinal template, Europhysics Letters 58, 5 (2002) 730 – 736.
20. V.Y. Vvedenskiy, E.N. Tokmakova, Model of the hysteresis loop of soft-magnetic amorphous alloys with the usage of a modified linear fractional function, Lett. Mater. 11, 2 (2021) 158 –163.
21. H. Kanter, F.L. Vernon Jr., High-Frequency Response of Josephson Point Contacts, Journal of applied physics 43, 7 (1972) 3174 – 3183.
22. T.S. Khaire, M.A. Khasawneh, W.P. Pratt Jr., N.O. Birge, Observation of spin-triplet superconductivity in Co-based Josephson junctions, Physical review letters 104, 13 (2010) 137002.
23. M. Eschrig, Spin-polarized supercurrents for spintronics, Physics Today 64, 1 (2011) 43 – 49.
24. M. Tanaka, M. Furuta, T. Ichikawa, et al., Generation of spin-polarized electronic currents using perpendicularly magnetized cobalt ferrite spin-filtering barriers grown on spinel-type-conductive layers, Applied Physics Letters 122, 4 (2023) 042401.
25. N.M. Shchelkachev, Critical current in superconducting quantum point contacts, Journal of Experimental and Theoretical Physics Letters 71 (2000) 504 – 507.
26. A. Vakhrushev, A. Fedotov, A. Sidorenko, Simulation of Multilayer Nanosystems Interface Formation Process for Spintronics, Key Engineering Materials 888 (2021) 57 – 65.
27. A.S. Sidorenko, R.A. Morari, V. Boian, et al., Hybrid nanostructures superconductor-ferromagnet for superconducting spintronics, Journal of Physics: Conference Series 1758, 1 (2021) 012037.
28. A.V. Vakhrushev, A.Yu. Fedotov, Yu.B. Savva, A.S. Sidorenko, Modeling the processes of atom structure formation of a superconducting spin valve, PNRPU Mechanics Bulletin 2 (2020) 16 – 27. (in Russian)
29. A.V. Vakhrushev, A.Yu. Fedotov, O.Yu. Severyukhina, A.S. Sidorenko, The influence of structure and local structural defects on the magnetic properties of cobalt nanofilms, Beilstein Journal of Nanotechnology 14, 1 (2023) 23 – 33.
30. J. Tranchida, S.J. Plimpton, P. Thibaudeau, A.P. Thompson, Massively parallel symplectic algorithm for coupled magnetic spin dynamics and molecular dynamics, Journal of Computational Physics 372 (2018) 406 – 425.
31. D.L. Ermak, H. Buckholz, Numerical integration of the Langevin equation: Monte Carlo simulation, Journal of Computational Physics 35, 2 (1980) 169 –182.
32. F. Xu, G. Li, J. Chen, et al., Unified framework of the microscopic Landau-Lifshitz-Gilbert equation and its application to skyrmion dynamics, Physical Review B 108, 14 (2023) 144409.
33. J.L. Garcia-Palacios, F.J. Lazaro, Langevin-dynamics study of the dynamical properties of small magnetic particles, Physical Review B 58, 22 (1998) 14937–14958.
34. M.I. Baskes, Modified embedded-atom potentials for cubic materials and impurities, Physical Review B 46, 5 (1992) 2727 – 2742.
35. S. Plimpton, Fast Parallel Algorithms for Short-Range Molecular Dynamics, Journal of Computational Physics 117, 1 (1995) 1–19.
36. Y. Henry, K. Ounadjela, L. Piraux, et al., Magnetic anisotropy and domain patterns in electrodeposited cobalt nanowires, The European Physical Journal B-Condensed Matter and Complex Systems 20 (2001) 35 – 54.
37. A.V. Prokaznikov, V.A. Paporkov, V.A. Chirikov, Features of the magneto-optical response of nanostructures formed under ion-beam surface treatment in different modes, Journal of Surface Investigation: X-Ray, Synchrotron and Neutron Techniques 16, 6 (2022) 1111–1120.
38. J.G. Guo, Y.P. Zhao, The size-dependent elastic properties of nanofilms with surface effects, Journal of Applied Physics 98, 7 (2005) 074306.
39. D. Choi, B. Son, T.H. Park, J. Hong, Controlled surface functionality of magnetic nanoparticles by layer-by-layer assembled nano-films, Nanoscale 7, 15 (2015) 6703 – 6711.
40. A.G. Nugumanov, D.I. Abdrakhmanov, R.R. Nugumanov, I.F. Sharafullin, Skyrmions in perforated magnetic film with Dzyaloshinskii–Moriya interaction, Lett. Mater., 15, 3 (2025) 176 –183.
41. E.N. Zanaeva, A.I. Bazlov, A.A. Kazakova. Structure and magnetic properties of amorphous alloys of the Fe-Co-Cr-B system with varying Fe/Co ratios, Lett. Mater. 15, 3 (2025) 220 – 226.